Computational Study on Combustion Characteristics of Various Samples of Pulverized Coal in a Dual Swirl Co-and Counter Combustor

Munamala Penchala Reddy[1], Hemachandra Reddy[1]

[1] JNTU College of Engineering, Anantapur, Andhra Pradesh, India

Abstract

Pulverized coal combustion is the primary method of generating thermal power in India. The combustion of pulverized coal is carried out in large furnaces. Improvement in the design and performances of these furnaces and detailed picture of its behaviors at different operating conditions can be efficiently assisted using computational fluid dynamics modeling. In the present work, we investigate the combustion and emissions characteristics of high-grade foreign and low-grade Indian coals using a dual swirl assisted (counter swirl configuration) pulverized coal combustion burner modeled with CFD. In addition, flame characteristics, flow patterns, and CO emissions are extensively discussed. Results indicate that low-grade Indian coals with high ash and moisture, IS2 and IS3, perform less well than high-grade foreign coals, IAS1 and SA1. As a result, low-grade Indian coals with high ash and moisture content will need a strong swirl and longer combustion chamber. As far as CO emissions are concerned, Indonesian coal IAS1 and Indian coal IS1 rank higher than the other coals. However, IS3 from India has the overall worst CO emission performance.

Keywords: Swirl combustion, Devolatilization, Moisture, Ash, Recirculation

IJSER

1. Introduction

A growing population and rapid industrialization are contributing to the high demand for electricity. Currently, fossil fuels such as coal and natural gas are the major fuel sources for power production. Coal resources are abundant in countries such as India, China, Indonesia, and Australia. India generates 60- 65% of its energy through thermal power plants using coal as the primary fuel. However, emissions from coal combustion, such as CO, NOx, particulate matter (PM), SOx, and heavy metals, accumulate in the atmosphere and lead to serious health and environmental problems [1–3]. In comparison to Chinese, Indonesian, and Australian coals, Indian coal contains a lot of moisture and ash. The combustion chemistry of coal is a highly complex phenomenon because it involves interactions between the gaseous phase and minerals as well as carbonaceous components [1,4–6]. As a result, a comprehensive study of coal combustion ignition chemistry is essential. The ignition delay phenomenon helps in the understanding of fuel's ignition characteristics. Reddy et al. [7] studied the effect of furnace temperature, oxygen concentration, and particle size on the ignition delay time of high moisture and high ash Indian coals, and a comparison has been made with Indonesian and South-African coals. Results show that Indian coal exhibits slower ignition characteristics compared to Indonesian and South-African coals, and its performance enhances with mixing with high-grade foreign coals. Results also highlighted that the increase in the furnace temperature and decrease in particle size decrease the ignition delay time of coal particles. Overcoming the high CO and NO_x emissions from coal-powered burners is a significant challenge. Emissions reduction techniques such as swirling, porous, and mild combustion are implemented to reduce CO and NOx emissions.

Sung and Choi [8] studied the effect of co and counter swirl configurations on the flame characteristics, heat release region, and internal recirculation zone behavior of dual swirl pulverized coal combustion. Sung and Choi [8] results suggest that the counter swirling flames

IJSER

exhibit a higher heat release rate and flame temperature is due to enhanced mixing, which results in an intensified combustion reaction between coal particles. Results also highlight that the internal recirculation zone area increases for conditions with high swirls, whereas it decreases for conditions with low swirls. A swirl flow generates an internal recirculation zone because of local pressure variations, and its shape and characteristics are dependent on burner working conditions and the nature of the swirl. Gu et al. [9] studied the effect of swirl intensity and particle motion on the NOx emission characteristics of pulverized coal combustion. Gu et al. [9] results highlight that the lower NOx emissions were observed for the higher effective time of the internal recirculation zone and particle penetration depth. The work of Ti et al. [10] studied the impact of outer secondary air cone length on the NOx emission characteristics of fuel-rich swirl-assisted pulverized coal combustion. Ti et al. [10] found that the increases in outer cone length increase the internal recirculation zone size, which in turn decreases the NOx emission. The NOx emission reduction in coal combustion can also be achieved by adding a De-NOx agent such as ammonia. Zhang et al. [11] numerically studied the effect of the co-firing ammonia ratio on the combustion and NOx emissions characteristics of pulverized coal in a swirl-assisted burner. Zhang et al. [11] found that the NOx and unburnt carbon significantly depends on the co-firing ammonia ratio. For the ammonia co-firing ratio of 10%, an increase in NOx and reduction in unburnt carbon and ammonia emissions is observed due to more intense combustion. However, for the ammonia co-firing ratio of greater than 10%, more unburned NH_3 and lesser NOx emissions is observed due to De-NOx characteristics of ammonia. Also, the co-firing ammonia ratio is greater than 40%, resulting in a long and thin flame rather than the normal swirl flame. This is because of the complete penetration of internal recirculation zone by high-velocity ammonia jet. The above-discussed studies have shown that modification in swirl types or intensity plays an essential role in NOx reduction, flow mixing, and flame stability.

IJSER

It is essential to have a detailed understanding of pulverized coal combustion characteristics to achieve low CO and NOx combustion technologies. Especially the burner or furnaces designed for Indian grade coals. Indian grade coals consist of high ash and moisture and lead to higher NOx and CO emissions than the foreign grade coals. In the present work, a computational fluid dynamics (CFD) analysis is performed to study the combustion and emissions characteristics of Indian grade coals in a dual swirl assisted pulverized coal combustion. The properties of Indian-grade coal are mentioned in Table 1. Furthermore, flame characteristics, flow mixing, CO emission behavior are extensively highlighted in work.

2. Numerical Methodology

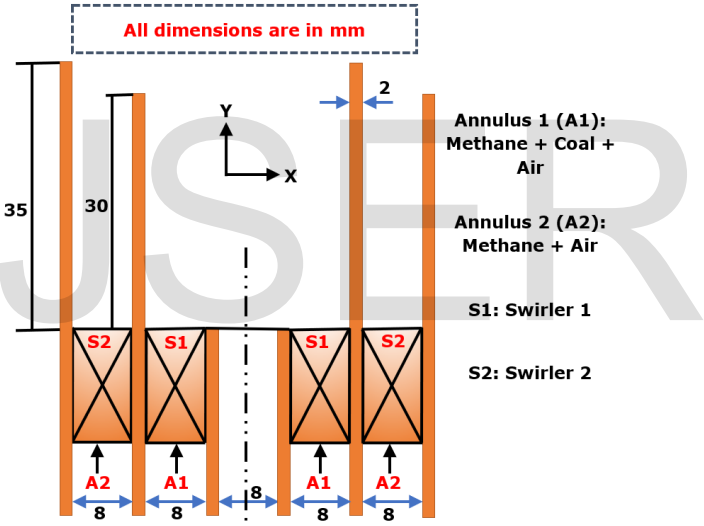

Figure 1: Schematic representation of computational domain.

The figure 1 shows the schematic description of the computational domain. The computational domain is considered from the work of Sung and Choi [8]. Three coaxial tubes containing dual axial swirlers are situated in a coaxial arrangement. The first and second swirlers were mounted respectively at annulus 1 (inner swirler, A1) and 2 (outer swirler, A2), as shown in Fig 1. Both inner and outer swirlers consist of six evenly spaced blades having a thickness of 2 mm inclined at 40, 60, and 80 to the combustor exit plane. In the inner annulus (A1), pulverized coal

particles are transported by a mixture of methane and air. The outer annulus (A2) is also supplied with a methane/air mixture. The Fig. 2 represents the mesh details of the combustor considered in the present study. The swirl number is calculated using the Eqn.1 [8]. Where the terms D_i and D_O represent the inner and outer diameter of the swirler. The Eqn. 1 shows that the swirl number (S_N) primarily depends on the inclination of the vane.

$$S_N = 0.666 \times \tan(\theta) \times \left[\frac{1-\left(\frac{D_i}{D_O}\right)^3}{1-\left(\frac{D_i}{D_O}\right)^2}\right] \quad (1)$$

The swirl number for the outer annular vane is considered as 0.71 and 4.79 corresponding to the vane inclination of 40^O and 80^O. The swirl number for the inner annular vane is considered as 1.3 corresponding to vane inclination of 60^O. In the burner, co- and counter swirl configurations are made feasible by controlling the inner swirler (S1) position. The angular position of the inner swirler (S1) is changed by varying the swirl vane angle from -60^O to 60^O. The swirl vane angle of -60^O results in a counter swirling motion. Mathematical modeling of coal combustion is challenging because it incorporates the combined interaction of 3-D fluid dynamics of gas-solid particles, heat transfer, turbulent interaction, and complicated heterogeneous and homogeneous chemical reactions [12]. The aerodynamic drag force depends mainly on the particle shape, and it significantly controls the motion of particles in the furnace. For these simulations, coal particles are assumed to be spherical in shape. A Lagrangian approach is adopted to track coal particle trajectories taking into account the turbulent dispersion. Equations 2 to 6 represent the differential governing equations for continuity, momentum, energy, and turbulent kinetic energy and dissipation rate. Further, swirl-assisted flow consists of complicated turbulent characteristics and rapid strains. The realizable k- ε turbulence model is used to analyze the turbulence interaction of flow with the improved wall treatment [13,14]. The Reynolds stresses are defined by this realizable k–ε

IJSER

model as shown in Eqn.7. Equations 9 and 10 represent the turbulent heat and mass flux. The values of constant σ_k , σ_ε , $C_{1\varepsilon}$, $C_{2\varepsilon}$, and C_m are considered as 1.0, 1.3, 1.44, 1.92, and 0.09. The values for turbulent Schmidt (Sc_{ta})and Prandtl (Pr_{ta}) number has been considered as 0.7 and 0.85. Similar values for these constants has also been considered in the study of Choi et al. [15,16]. Solution of the momentum equations in the Cartesian system as mentioned in Eqns. 11 and 12 resulted in the trajectory of a discrete phase particle. Moreover, the stochastic tracking model is used to consider particle dispersion caused by fluid turbulence [17]. In the stochastic tracking model, if the mean fluid velocity is exchanged with the instantaneous fluid velocity, the particle turbulence dispersion can be determined [15]. Heat is transferred primarily through thermal radiation in pulverized coal combustion because of intense particle radiation. Improved computational calculations of heat transfer in such systems require a highly accurate thermal radiation model. Radiation heat transfer was modeled using the P-1 radiation model. Equations 13 and 14 were used to calculate the radiation heat flux. The gaseous mixture emissivity is defined using the grey gas model weighted sum. Equations 15 and 16 are used to represent the emissivity and absorption coefficient. The reacting flow simulations are performed using the species transport model.

IJSER

$$\frac{\partial(\rho U)}{\partial x}+\frac{\partial(\rho V)}{\partial y}+\frac{\partial(\rho W)}{\partial z}=0 \tag{2}$$

$$\frac{\partial(\rho U U_i)}{\partial x}+\frac{\partial(\rho V U_i)}{\partial y}+\frac{\partial(\rho W U_i)}{\partial z} = \frac{\partial}{\partial x}\left(\mu\frac{\partial U_i}{\partial x}\right)+\frac{\partial}{\partial y}\left(\mu\frac{\partial U_i}{\partial y}\right)+\frac{\partial}{\partial z}\left(\mu\frac{\partial U_i}{\partial z}\right)-\frac{\partial p}{\partial x_i}+S_i \tag{3}$$

$$\frac{\partial(\rho U T)}{\partial x}+\frac{\partial(\rho V T)}{\partial y}+\frac{\partial(\rho W T)}{\partial z}=\frac{\partial}{\partial x}\left(\frac{k_h}{c_p}\frac{\partial T}{\partial x}\right)+\frac{\partial}{\partial y}\left(\frac{k_h}{c_p}\frac{\partial T}{\partial y}\right)+\frac{\partial}{\partial z}\left(\frac{k_h}{c_p}\frac{\partial T}{\partial z}\right)+S_q \tag{4}$$

$$\frac{\partial(\rho Uk)}{\partial x}+\frac{\partial(\rho Vk)}{\partial y}+\frac{\partial(\rho Wk)}{\partial z} \tag{5}$$

$$=\frac{\partial}{\partial x}\left(\left(\mu+\frac{\mu_{tk}}{\sigma_k}\right)\frac{\partial k}{\partial x}\right)+\frac{\partial}{\partial y}\left(\left(\mu+\frac{\mu_{tk}}{\sigma_k}\right)\frac{\partial k}{\partial y}\right)$$

$$+\frac{\partial}{\partial z}\left(\left(\mu+\frac{\mu_{tk}}{\sigma_k}\right)\frac{\partial k}{\partial z}\right)+S_k-\rho\varepsilon$$

$$\frac{\partial(\rho U\varepsilon)}{\partial x}+\frac{\partial(\rho V\varepsilon)}{\partial y}+\frac{\partial(\rho W\varepsilon)}{\partial z} \tag{6}$$

$$=\frac{\partial}{\partial x}\left(\left(\mu+\frac{\mu_{tk}}{\sigma_\varepsilon}\right)\frac{\partial k}{\partial x}\right)+\frac{\partial}{\partial y}\left(\left(\mu+\frac{\mu_{tk}}{\sigma_\varepsilon}\right)\frac{\partial k}{\partial y}\right)$$

$$+\frac{\partial}{\partial z}\left(\left(\mu+\frac{\mu_{tk}}{\sigma_\varepsilon}\right)\frac{\partial k}{\partial z}\right)+C_{1\varepsilon}\frac{S_k\varepsilon}{k}-\frac{C_{2\varepsilon}\rho\varepsilon^2}{k}$$

IJSER

$$-\rho\overline{U'_\iota U'_J}=\mu_{ta}\left(\frac{\partial U_i}{\partial x_j}+\frac{\partial U_j}{\partial x_i}\right)-\frac{2}{3}\rho k\beta_{ij} \tag{7}$$

$$\mu_{ta}=\frac{\rho C_m k^2}{\varepsilon} \tag{8}$$

$$\rho c_p\overline{U'_\iota T'}=-\delta_t\frac{\partial T}{\partial_{x_i}}=-c_p\frac{\mu_{ta}}{Pr_{ta}}\frac{\partial T}{\partial x_i} \tag{9}$$

$$\rho\overline{U'_\iota C'}=-\rho D_{ct}\frac{\partial C}{\partial x_i}=\frac{\mu_{ta}}{Sc_{ta}}\frac{\partial C}{\partial x_i} \tag{10}$$

$$\frac{d\overrightarrow{U_{pa}}}{dt} = \frac{18\mu}{\rho_{pa} D_{pa}^2} \frac{C_d Re_{pa}}{24} \left(\vec{U} - \overrightarrow{U_{pa}}\right) + \frac{\vec{g}\left(\rho_{pa} - \rho\right)}{\rho_{pa}} \tag{11}$$

$$Re_{pa} = \frac{\rho D_{pa} \left|\overrightarrow{U_{pa}} - \vec{U}\right|}{\mu} \tag{12}$$

$$Q_{ra} = -\frac{1}{3(b + \sigma_{sc}) - F\sigma_{sc}} \nabla I \tag{13}$$

$$\nabla . \left(\frac{\nabla I}{3(b + \sigma_{sc}) - F\sigma_{sc}}\right) - bI + 4bl^2 \sigma T^4 = 0 \tag{14}$$

$$\varepsilon = \sum_{j=0}^{G} b_{\varepsilon,j}(T)(1 - e^{-K_j pm}) \tag{15}$$

$$b_{\varepsilon,j} = \sum_{r=1}^{R} w_{\varepsilon,j,r} T^{r-1} \tag{16}$$

IJSER

Coal devolatilization is studied using the single rate devolatilization model based upon the eddy dissipation or finite rate. The decomposition of volatile substances from the pulverized coal combustion is considered according to the below reactions. The coefficients z, x, y, t, and m are calculated using the ultimate and proximate analysis.

$$C_z\, H_x O_y N_t S_m + \left(\frac{z}{2} + m - \frac{y}{2}\right) O_2 \rightarrow zCO + 0.5zH_2\, O + mSO_2$$

$$CO + \frac{1}{2} O_2 \rightarrow CO_2$$

$$H_2 + \frac{1}{2} O_2 \rightarrow H_2 O$$

Thermal decomposition of pulverized coal particles using the model of single rate devolatilization can be understood using Eqn. 17, and devolatilization rate can be expressed using the Eqn. 18. Tables 1 and 2 show the details of coals and operating conditions considered for the simulations.

$$\frac{dm_{pa}}{dt} = -k_{rd}\left[m_{pa} - \left(1 - v_{i,o}\right)m_{pa,i}\right] \quad (17)$$

$$k_{rd} = A_p e^{\frac{E_{act}}{RT_{pa}}} \quad (18)$$

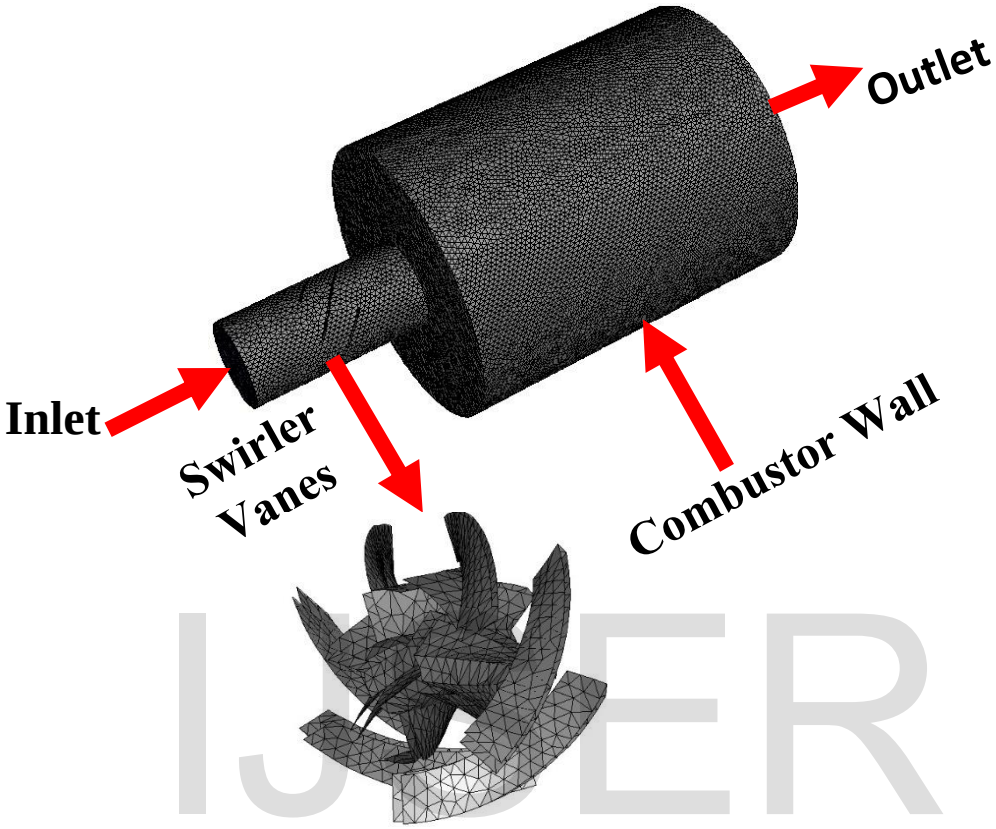

IJSER

Figure 2: Mesh of the modeled counter swirl assisted coal combustor with 2072261 cells.

2 Model Validation

In the present work, model validation is performed using the numerical results of Sung and Choi [8]. A variation of radial profiles of mean axial velocity at y/d ratios of 0.25, 1.0, and 2.0 is shown in Fig 3.

Sung and Choi [8] considered the swirl number of 0.71 and 4.79 for both co and counter-flow arrangements. However, for model validation, we have considered the result for the counter-flow swirl condition of 0.79. The valley-bottom effect observed for counter-swirling

conditions is due to the presence of the merged stagnation point for negative axial mean velocity distributions.

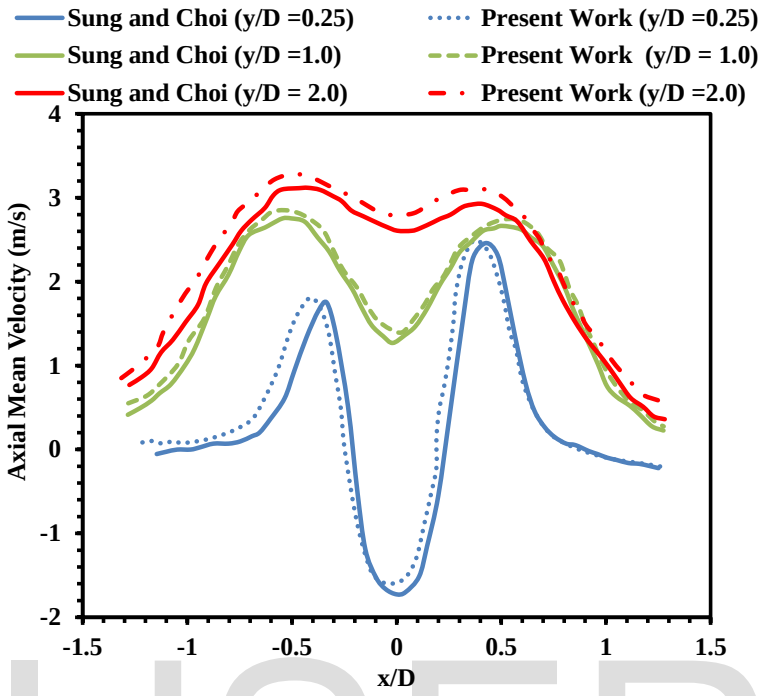

Figure 3: Variation of axial mean velocity with x/D at different y/D ratio and counter swirl number of 0.71.

IJSER

3 Results and Discussion

3.2 Ignition Delay Time Variation of the Different coal Samples

The characteristics of coal are essential factors in determining different coal combustion properties, such as coal-burning rate, energy release rate, and ignition temperature. The kinds of hydrocarbons present in coal significantly impact these combustion characteristics. A fuel's ignition property is closely related to its flame stability. Therefore, it is necessary to examine the ignition behavior of fuels. The flame's characteristics are strongly influenced by the ignition delay time in pulverized coal combustion. Pulverized coal's ignition characteristics are affected by particle size, moisture, and ash content. In Fig. 4, the ignition delay time variation of three Indian coals (IS1, IS2, and IS3), one Indonesian and African coals (IAS1 and SA1) with furnace

temperature are shown at an oxygen concentration of 12% and particle size ranges from 12 to 85µm. The graph shows that with increasing furnace temperature, the ignition delay time of pulverized coal mixtures decreases. The ignition delay time of a mixture is also reduced when coal particle size is reduced. More extensive understanding of ignition delay time modeling using different coal and approaches can be found in the authors previous work [7] .

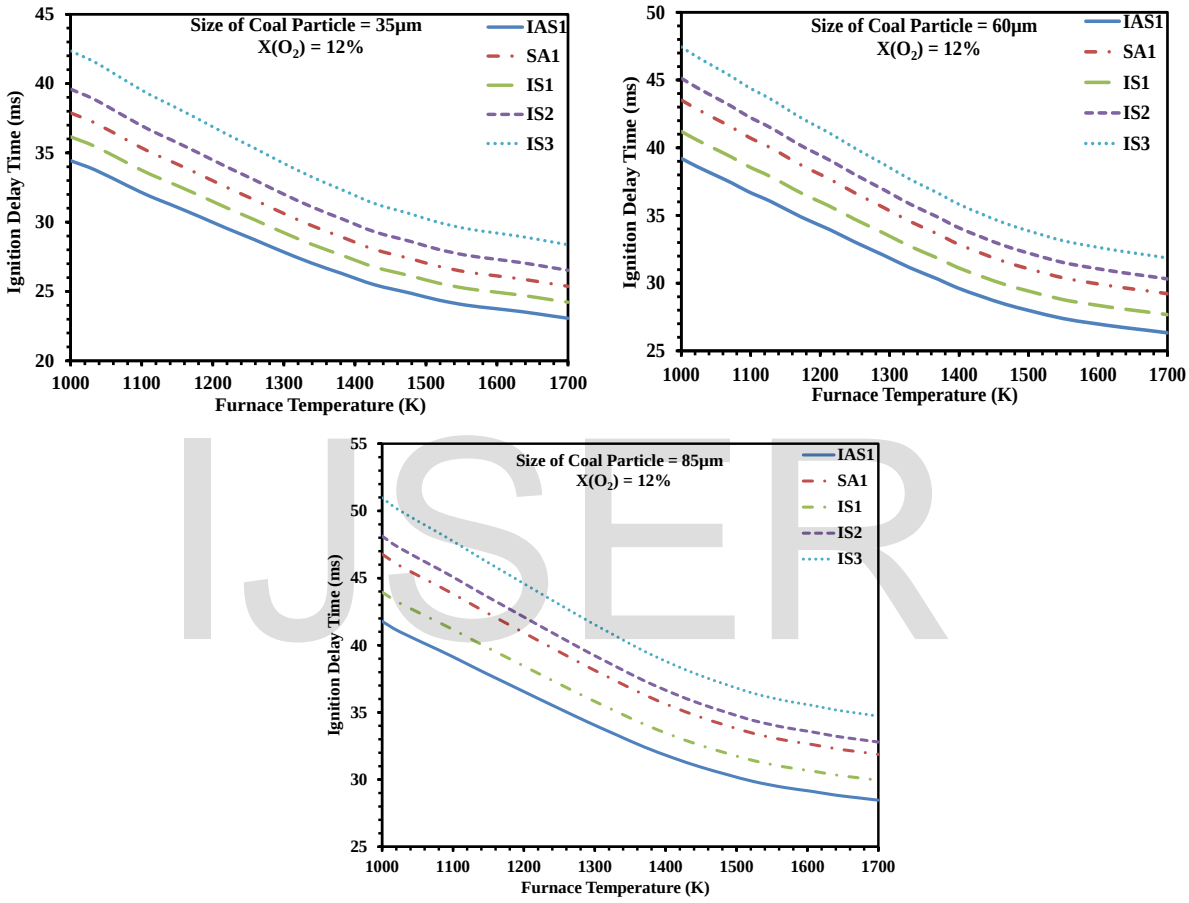

Figure 4: Variation of ignition delay time with furnace temperature of different coals at oxygen concertation of 12% and particle size of 35, 60, and 85µm.

3.3 Variation of Flow Pattern

Understanding axial velocity distribution plays an influential role in determining the flow patterns inside the combustor. Figure 5 shows the variation of axial velocity at distances of Z = 0.05, 0.1, and 0.15m. A valley bottom is found for negative velocity distributions. It appears

that two stagnation points cause a mountain peak in a positive velocity distribution. At Z=0.05m, higher peaks for velocity variation are observed compared to Z= 0.1 and Z=0.15 m. Overall similar trends are observed for velocity variation for all three cases.

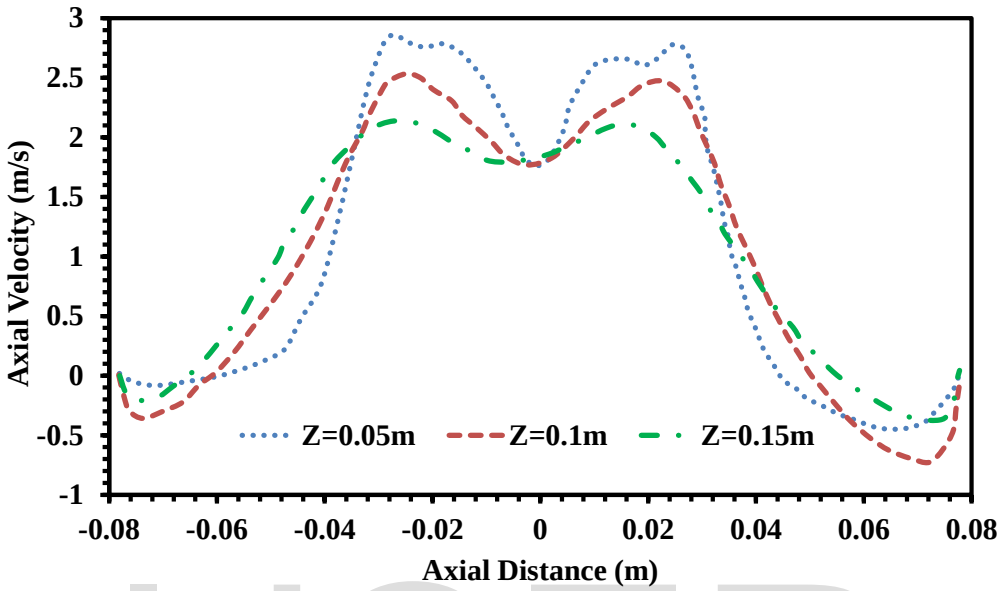

Figure 5: Variation of axial velocity at different Z locations.

IJSER

3.4 Variation of Temperature

Figure 6 shows the variation of temperature contours for the different coal types considered in table 1. The coal mixture inlet temperature and pressure are considered as the 400K and 1 atm. For comparison, three low-quality Indian coals (having high ash and high moisture) and one South African and one Indonesian coal are considered. Figure 6 shows that the Indonesian coal (IAS1) shows better ignition characteristics than the other coals considered in this work. In the case of IAS1, a more distributed flame is observed inside the burner. However, a less distributed flame appearance is observed for the Indian standard coals IS2 and IS3.

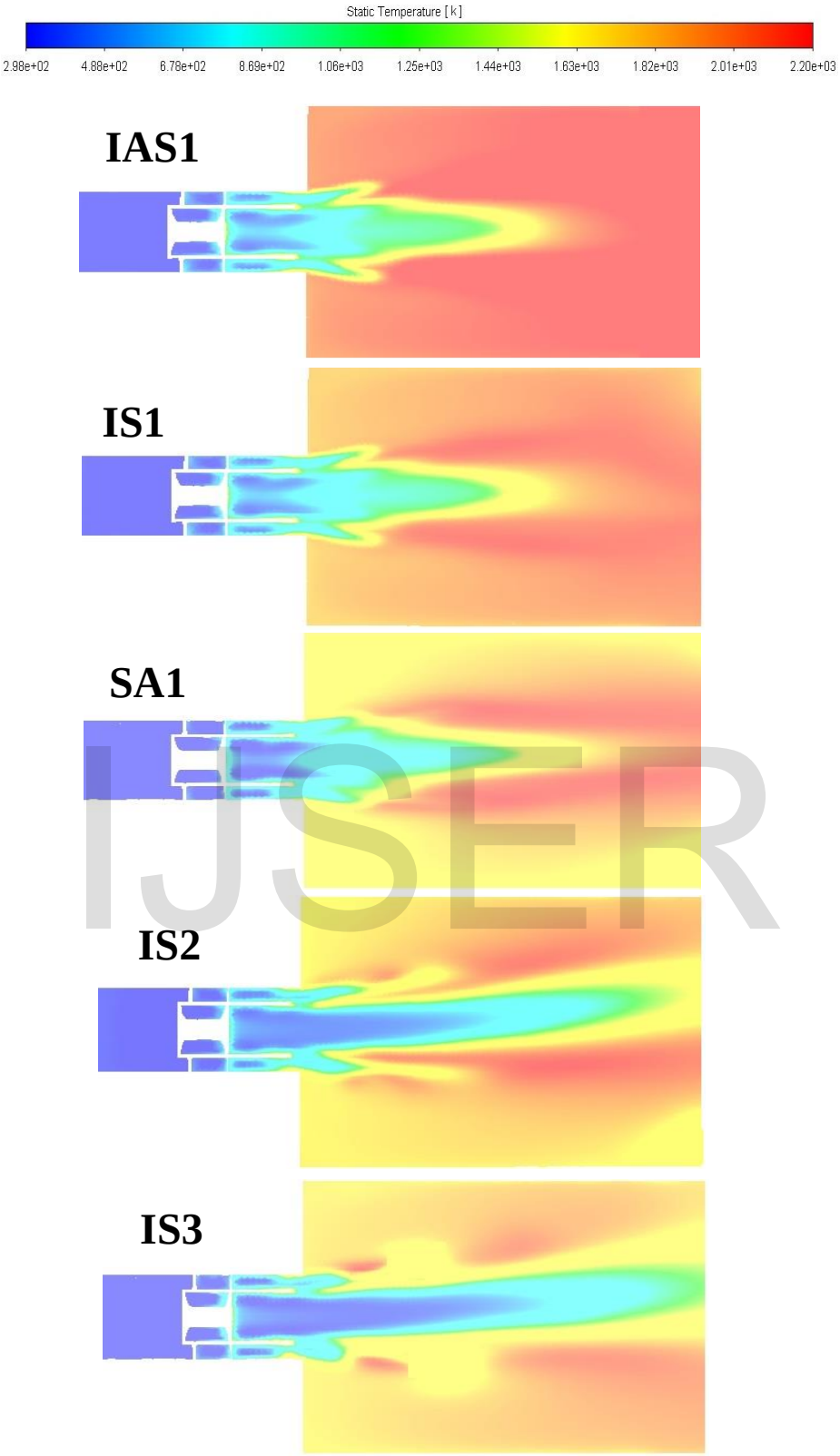

IJSER

Figure 6: Temperature variation contours for different coals considered in the present study.

Furthermore, the flame location shifted more downstream in IS2 and IS3 compared to high standard IAS1 coals. The Indian coals IS2 and IS3 conation high ash and high moisture compared to Indonesian coals (IAS1) and South African coals (SA1). Therefore, Indian coals will need a higher combustor length to compare fine grade foreign coals due to the presence of high ash and high moisture. The higher residence time will need in the combustion of high ash and high moisture coals.

3.5 CO Variation

IJSER

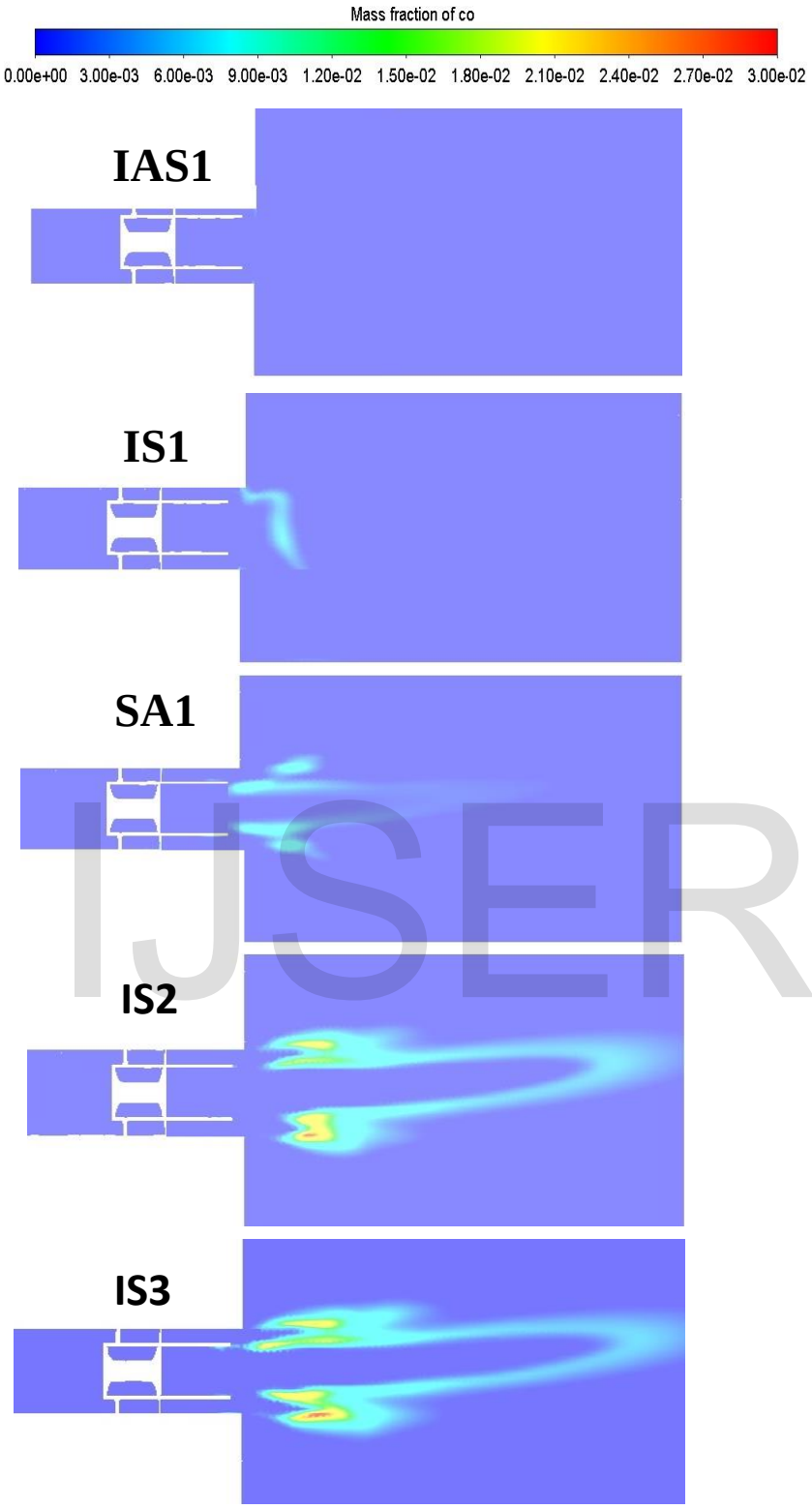

IJSER

Figure 7: CO variation contours for different coals considered in the present study

Figure 7 shows the variation of temperature contours for the different coal types considered in the present work. A heterogeneous reaction occurs between the volatile substances produced from the solid coal particle and the solid char (C_{Solid}). The heterogeneous reactions between char and volatiles involve the following three-step surface reactions. Kinetics rates for three-step heterogeneous reactions have been considered from the work of Vascellari and Cau [18].

$$C_{Solid} + \frac{1}{2}O_2 \rightarrow CO \qquad \text{(Ra1)}$$

$$C_{Solid} + CO_2 \rightarrow 2CO \qquad \text{(Ra2)}$$

$$C_{Solid} + H_2O \rightarrow CO + H_2 \qquad \text{(Ra3)}$$

The above mention reactions Ra1, Ra2, and Ra3 are the main pathway for CO formation in coal combustion. In terms of CO emissions, the Indonesian coals IAS1 shows better performance than the other coals. While, the Indian standard coals IS3 shows the worst performance for CO emissions.

IJSER

4 Conclusion

Despite the significant growth in non-conventional power generation in the past few years, coal remains the primary source of electricity in developing countries like India. An essential goal of coal-fired power plants is to achieve nearly efficient combustion with the least amount of harmful emissions possible. In order to prevent the waste of natural resources, as well as reduce fossil fuel's adverse impact on human health and climate change, therefore, a better understanding of coal combustion is essential. In this study, a dual swirl assisted (counter swirl configuration) pulverized coal combustion burner is modeled with CFD to investigate the combustion and emissions characteristics of high-grade foreign and low-grade Indian coals. Additionally, flame characteristics, flow patterns, and CO emissions are explored extensively. Results suggest that low-grade Indian coals with high ash and high moisture IS2 and IS3

perform poorer than high-grade foreign coals IAS1 and SA1. The Indian grade coals IS3 shows similar flame characteristics to IAS2 due to lesser ash and moisture content. Therefore, low-grade Indian coals having high ash and moisture content will require a strong swirl and higher combustor length for better combustion. In the case of CO emissions, Indonesian coal IAS1 and Indian coals IS1 shows better performance than the other coals. The Indian coal IS3 shows the worst CO emissions performance.

Nomenclature

U= Velocity of particle

k_h = Forward rate reaction constant

S_k = Kinetic energy of turbulence generated by mean velocity gradients

μ_{ta} = Turbulent viscosity

k = Turbulent kinetic energy

C_m = Constant

ε = Turbulent dissipation

δ_t = Turbulent heat conductivity

D_{ct} = Turbulent diffusion coefficient

Pr_{ta} = Turbulent Prandtl number

Sc_{ta} = Turbulent Schmidt number

D_{pa} = Diameter of particle

U_{pa} = Velocity of particle

ρ_{pa} = Density of particle

Re_{pa} = Reynolds number of particle

I = Incident radiation

b= Coefficient of absorption

$b_{\varepsilon,j}$ = J^{th} fictitious grey gas emissivity weighting factor

$w_{\varepsilon,j,r}$ = Temperature polynomial coefficient for gas emissivity

IJSER

F = Function coefficient of linear-anisotropic phase

σ_{sc} = Coefficient of scattering

K_j =jth grey gas absorption coefficient

p= Partial pressure summation of all absorbing gases

T= Gas temperature

Q_{ra} = Radiation heat flux

m_{pa} = Mass of particle (kg)

k_{rd} = Devolatilization rate

$v_{i,o}$ = Particle initial volatile fraction

$m_{pa,i}$ = Particle initial mass (kg)

A_p = Pre-exponential factor

E_{act} = Activation energy

R = Universal gas constant

T_{pa} = Temperature of particle

IJSER

References

[1] S. Yadav, S.S. Mondal, A complete review based on various aspects of pulverized coal combustion, Int. J. Energy Res. 43 (2019) 3134–3165. https://doi.org/10.1002/er.4395.

[2] A.S. Singh, S. Mohapatra, R. Boyapati, A.M. Elbaz, S.K. Dash, W.L. Roberts, V.M. Reddy, Chemical Kinetic Modeling of the Autoignition Properties of Ammonia at Low–Intermediate Temperature and High Pressure using a Newly Proposed Reaction Mechanism, Energy & Fuels. 35 (2021) 13506–13522. https://doi.org/10.1021/acs.energyfuels.1c01243.

[3] A.S. Singh, S.K. Dash, V.M. Reddy, Chemical kinetic analysis on influence of hydrogen enrichment on the combustion characteristics of ammonia air using newly proposed reaction model, Int. J. Energy Res. 46 (2021) 6144–6163. https://doi.org/10.1002/er.7554.

[4] J.K. Kim, H.D. Lee, Combustion Characteristics of High Moisture Indonesia Coal as a Pulverized Fuel at Thermal Power Plant, J. Chem. Eng. Japan. 43 (2010) 704–712. https://doi.org/10.1252/jcej.10we008.

[5] S.S. Makgato, E.M.N. Chirwa, Characteristics of thermal coal used by power plants in Waterberg region of South Africa, Chem. Eng. Trans. 57 (2017) 511–516. https://doi.org/10.3303/CET1757086.

[6] S. Golgiyaz, M.F. Talu, M. Daşkın, C. Onat, Estimation of excess air coefficient on coal combustion processes via gauss model and artificial neural network, Alexandria Eng. J. (2021). https://doi.org/10.1016/j.aej.2021.06.022.

[7] M. Penchala Reddy, A. Shankar Singh, V. Mahendra Reddy, A. Elwardany, H. Reddy, Computational analysis of influence of particle size, oxygen concertation, and furnace temperature on the ignition characteristics of pulverized high ash and high moisture coal particle, Alexandria Eng. J. 61 (2022) 6169–6180. https://doi.org/10.1016/j.aej.2021.11.047.

[8] Y. Sung, G. Choi, Non-intrusive optical diagnostics of co- and counter-swirling flames in a dual swirl pulverized coal combustion burner, Fuel. 174 (2016) 76–88. https://doi.org/10.1016/j.fuel.2016.01.011.

[9] M. Gu, M. Zhang, W. Fan, L. Wang, F. Tian, The effect of the mixing characters of primary and secondary air on NO x formation in a swirling pulverized coal flame, Fuel. 84 (2005) 2093–2101. https://doi.org/10.1016/J.FUEL.2005.04.019.

[10] S. Ti, Z. Chen, Z. Li, X. Zhang, H. Zhang, G. Zou, L. Zeng, Q. Zhu, Effects of the outer secondary air cone length on the combustion characteristics and NOx emissions of the swirl burner in a 0.5 MW pilot-scale facility during air-staged combustion, Appl. Therm. Eng. 86 (2015) 318–325.

IJSER

https://doi.org/10.1016/j.applthermaleng.2015.04.021.

[11] J. Zhang, T. Ito, H. Ishii, S. Ishihara, T. Fujimori, Numerical investigation on ammonia co-firing in a pulverized coal combustion facility: Effect of ammonia co-firing ratio, Fuel. 267 (2020). https://doi.org/10.1016/j.fuel.2020.117166.

[12] R. Viskanta, M.P. Mengüç, Radiation heat transfer in combustion systems, Prog. Energy Combust. Sci. 13 (1987) 97–160. https://doi.org/10.1016/0360-1285(87)90008-6.

[13] S. Chen, Z. Liu, J. Liu, J. Li, L. Wang, C. Zheng, Analysis of entropy generation in hydrogen-enriched ultra-lean counter-flow methane-air non-premixed combustion, Int. J. Hydrogen Energy. (2010). https://doi.org/10.1016/j.ijhydene.2010.08.048.

[14] M. Gu, M. Wang, X. Chen, J. Wang, Y. Lin, H. Chu, Numerical study on the effect of separated over-fire air ratio on combustion characteristics and NOx emission in a 1000 MW supercritical CO2 boiler, Energy. 175 (2019) 593–603. https://doi.org/10.1016/j.energy.2019.03.111.

[15] M. Choi, Y. Park, X. Li, K. Kim, Y. Sung, T. Hwang, G. Choi, Numerical evaluation of pulverized coal swirling flames and NOx emissions in a coal-fired boiler: Effects of co- and counter-swirling flames and coal injection modes, Energy. 217 (2021) 119439. https://doi.org/10.1016/j.energy.2020.119439.

[16] Z. Li, Z. Miao, Y. Zhou, S. Wen, J. Li, Influence of increased primary air ratio on boiler performance in a 660 MW brown coal boiler, Energy. 152 (2018) 804–817. https://doi.org/10.1016/j.energy.2018.04.001.

[17] F. Ren, Z. Li, L. Zeng, Z. Chen, Q. Zhu, Numerical simulation of flow, combustion, and NO x emission characteristics in a 300 MW down-fired boiler with different OFA

IJSER

ratios, Numer. Heat Transf. Part A Appl. 62 (2012) 231–249. https://doi.org/10.1080/10407782.2012.691062.

[18] M. Vascellari, G. Cau, Numerical simulation of pulverized coal oxy-combustion with exhaust gas recirculation, Proc. CCT2009 4th Int. Conf. Clean Coal Technol. Germany (2009).

IJSER